Microstructure and tribological properties of VS_x / TiO_2 composite layers in-situ prepared on TC4 alloy

Q. Li, J. Shang*, G.Y. Gu
Liaoning University of Technology, Jinzhou, 121000, Liaoning Province, China

The VS_X/TiO_2 composite layer was successfully prepared by adding Na_2S and Na_3VO_4 into electrolytes through micro-arc oxidation (MAO) method. The structure, morphology and tribological properties were analyzed by X-ray diffraction, scanning electron microscopy and 3D true color microscopy. The results show that when the concentration of Na_2S is 10-20 g/L, the thickness of VS_x/TiO_2 composite layer is the thickest, and the friction coefficient and volume wear are the lowest. The VS_x/TiO_2 composite layer in-situ prepared by MAO can improve the tribological properties of TC4 alloy at high temperature.

(Received September 15, 2023; Accepted January 12, 2024)

Keywords: Micro arc oxidation, VS_x/TiO_2 composite layer, Titanium alloy, Microstructure and tribological properties

1. Introduction

Titanium alloy are mainly divided into α-type titanium alloy, β-type titanium alloy and (α + β) type titanium alloy [1-4]. Titanium alloys have the advantages of light weight, high heat resistance, high strength and good corrosion resistance [5-9], and they are widely used in aerospace, ship, medical and other fields [10-14]. But due to poor oxidation and wear resistance [15-19], it is inevitable to be limited in the applications.

At present, the main methods to improve the wear resistance of titanium and its alloys are ion implantation, MAO and laser surface treatment [20-22]. The preparation of MAO layers are mainly deepened on the interaction between the electrical parameters and electrolyte solution. In order to decrease the porosity and improve the wear resistance of MAO layers, many researchers have studied the adding second-phase particles, such as MgO [23], Al_2O_3 [24], MoS_2 [25] to form a composite layer. However, the new phase generated by the second phase particles is either insufficient to improve the wear resistance, or has no practical effect on removal from the electrolyte, so the second phase particles addition is often complicated [26]. Therefore, the composite layer in-situ prepared during MAO process can be tried to play a self-lubricating role.

In this experiment, a composite layer containing VS_x/TiO_2 phase was expected to prepare by adding Na_2S into electrolyte containing Na_3VO_4 mainly. The effects of Na_2S concentration on the microstructure and tribological behavior are stuied. This work is aiming at to find a new method to improve wear resistance of TC alloy.

2. Experimental procedure

The TC4 substrate was polished with 120~1000 # sandpaper and ultrasonically cleaned with an ultrasonic cleaner. In this experiment, WHD-30 equipment was used for MAO treatment. The electrolyte was mainly composed of 2 g/L NaF + 6 g/L Na_3PO_4 + 4 g/L Na_3VO_4, and 0 g/L, 10 g/L, 20 g/L and 30 g/L Na_2S were added into the main salt solution. The MAO electrical parameters were as follows. The current density was 11 A/dm^2, operating frequency was 500 Hz; working duration was 30 min. The Axio Scope A1 Zeiss metallographic microscope is used to measure the thickness of layers. The surface roughness was obtained by HYBRD C3 true color

* Corresponding author: shangbahao@163.com
https://doi.org/10.15251/DJNB.2024.191.107

confocal microscope. The phase analysis of the layers was characterized by D/max-2500/pc diffractometer. The porosity and elemental composition of the layers were analyzed by Zeiss SIGMA 500 field emission scanning electron microscope and AZtec X-Max energy dispersive spectrometer. The Image J software was used to calculate the porosity. The wear resistance of the layers was tested by HT-100 high temperature friction and wear tester and the test parameters were as follows. The The Si_3N_4 ball was selected as the couple. Th test temperature was 600 °C; load is 10 N, rotational speed is 535 rpm and sliding duration was 20 min.

3. Results and analysis

From Fig.1, it can be seen that with the increase of Na_2S concentration, the surface morphology of the MAO layer surface changes significantly. When the concentration of Na_2S is 0 g/L, a large number of holes and cracks appear on the surface. When the Na_2S content is 10 g/L, the cracks on the surface disappear and the pore density decreases. When the Na_2S content is increased to 20 g/L, the MAO layer surface appears discontinuous layered structure and the pore diameter is further reduced, and only large pores exist on the discontinuous layer. When the Na_2S content is 30 g/L, the size and number of pores and cracks on the surface decrease to the minimum.

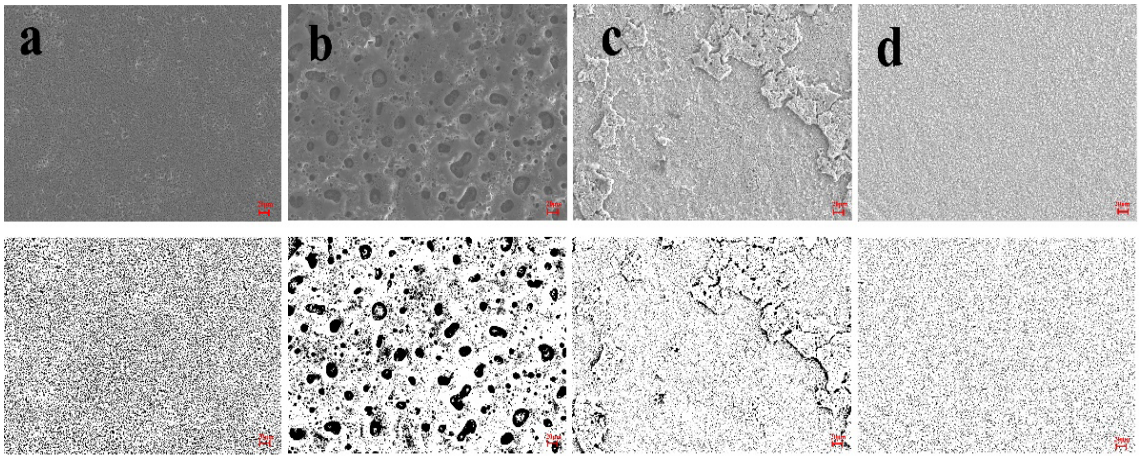

Fig. 1. The surface morphology and pore size distribution of different Na_2S content (a: 0 g/L, b: 10g/L, c: 20 g/L, d: 30 g/L).

The surface roughness of the MAO layer is mainly determined by the degree of uplift of the discharge sediment and the depression of discharge micropores. Fig.2 is the statistics of the surface roughness of MAO layer (Ra: arithmetic average roughness; Rp: maximum peak height; Rv: maximum valley peak height; Rz: average peak-valley depth; Rq: root mean square roughness). It can be seen from Fig.2 that surface roughness of the MAO layer changes significantly with the increase of Na_2S concentration. When the Na_2S concentration increases to 30 g/L, the five parameters reach the lowest at the same time.

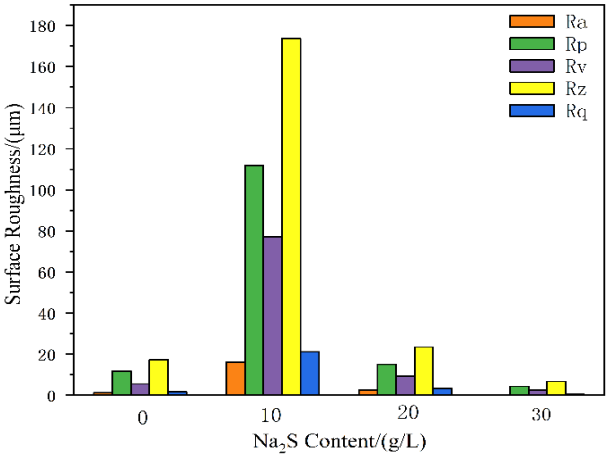

Fig. 2. Surface roughness statistics of MAO coatings with different Na_2S content.

It can be seen from Fig.3 that the porosity and the thickness of the film have the same change rule. When the concentration of Na_2S is 0 g/L, the porosity of MAO layer is up to 15.8 %. When the Na_2S content is 30 g/L, the porosity is only 10.77 %. When the content of Na_2S is 10 g/L, it has a negative effect on the porosity of MAO layer. However, when the Na_2S content reaches 20-30 g/L, the growth of MAO layer is inhibited, which leads to the thinnest MAO layer with the best flatness and the lowest porosity. Analysis from the film thickness. When the Na_2S content is 30 g/L, the growth of MAO layer is inhibited, and the average thickness is only 13.243 μm. When the Na_2S content is 10 g/L, the average thickness of the MAO layer reaches a maximum of 61.392 μm. Combined with Fig.2, it can be seen that the flatness of the MAO layer is poor when the thickness is thick. This is because the increase of Na_2S content reacts with Na_3VO_4 in the solution, and the generated VS_2 increases the thickness of MAO layer to a certain extent. The sharp decrease of MAO thickness at 20 g/L may be related to the change of solution conductivity. The excessive Na_2S greatly increased the resistance of the solution and reduced the voltage, resulting in a decrease in energy density and inhibiting the growth of the MAO layer.

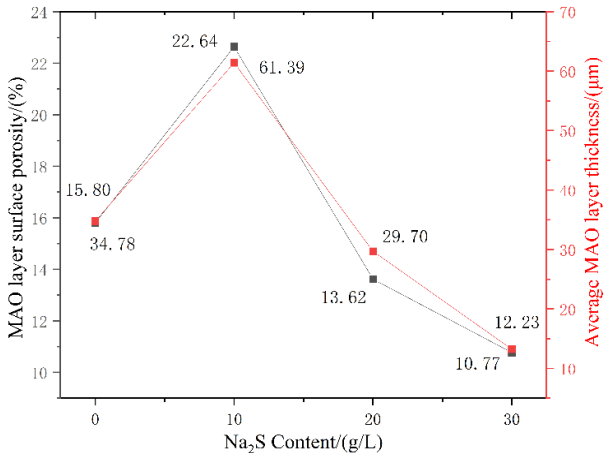

Fig. 3. Porosity and cross-sectional thickness of MAO layer under different Na_2S content.

It can be seen from Fig.4 that the addition of different concentrations of Na_2S also had a significant effect on the operating voltage of the MAO layer. When Na_2S was not added, the voltage increased sharply with the MAO reaction, and reached the peak at 300 s. At this time, it should be the stage I of micro-arc oxidation, that is, the breakdown stage. At this time, the voltage of 350 V is the stable reaction stage. With the gradual increase of Na_2S content, the working

voltage in the MAO process is gradually reduced. When the concentration is 10 g/L, the working voltage is 300 V. At this time, the micro-arc discharge energy is sufficient, so the MAO thickness is the thickest, but large-diameter pores appear.

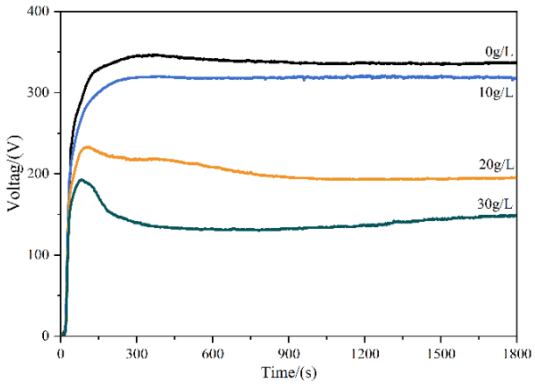

Fig. 4. The MAO layer reaction voltage of different Na_2S content.

At 20 g/L, the working voltage is maintained at about 200 V, which is already the critical voltage required for MAO. Therefore, the MAO layer is thin but the surface quality is improved. When the concentration of Na_2S exceeds 20 g/L, the spark discharge phenomenon has not been observed by the naked eye, indicating that the spark discharge is very weak at this time. The gradually reduced working voltage shows that Na_2S has a certain inhibitory effect on the micro-arc oxidation process. After more than 20 g/L, the working voltage will be lower than 200 V, which is lower than the high voltage requirement of MAO in the traditional sense.

From Fig.5, it can be seen that the MAO layer is mainly composed of Anatase-TiO_2, Rutile-TiO_2, Ti, and a small amount of VS_x phase. It can be seen that the Anatase-TiO_2 diffraction peak at about $2\theta = 24$ ° gradually decreases with the increase of Na_2S content, and the Rutile-TiO_2 diffraction peak gradually increases, which is because Na_2S promotes the growth of MAO layer. It leads to the decrease of thermal conductivity of the film and promotes the transformation of room temperature stable Anatase to high temperature stable Rutie. At the same time, it can be seen that the diffraction peak of Ti matrix at $2\theta = 38$ ° and $2\theta = 40$ ° began to increase when the Na_2S content was 20 g/L, indicating that the thickness of MAO layer began to decrease at this time. When the content of Na_2S is 30 g/L, the diffraction intensity of Ti matrix continues to increase because excessive Na_2S inhibits the growth of MAO layer, and the diffraction intensity is greatly affected by the matrix.

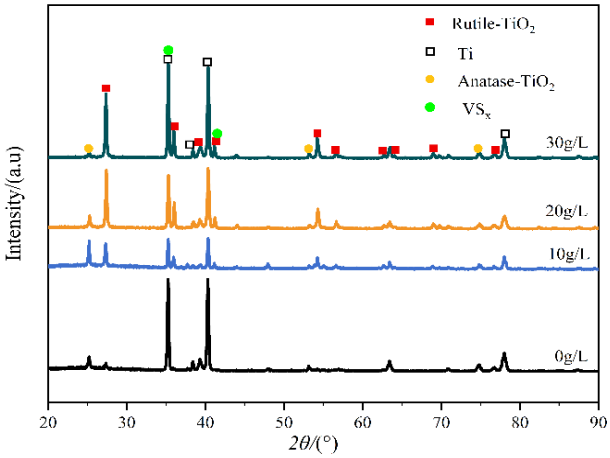

Fig. 5. X-ray diffraction analysis of MAO layer with different Na_2S content.

It can be seen from Fig.6 that the MAO layers with different Na_2S contents have similar composition elements. 0 g/L is mainly composed of four elements: Ti, O, V and Na. Among them, O and Ti elements constitute the main element composition in the MAO layer, and Ti element is mainly derived from the matrix and TiO_2. The O element comes from the deposition of oxides such as TiO_2 and SiO_2, and the V element mainly comes from the Na_3VO_4 existing in the electro-hydraulic and a small amount of elements in the matrix. The Na element comes from electrolytes such as Na_2F and Na_3VO_4. Although there is no very obvious VS_x phase in the XRD pattern, the appearance of V element in the SEM surface scan indicates that there may be VS_x phase on the surface of the MAO layer.

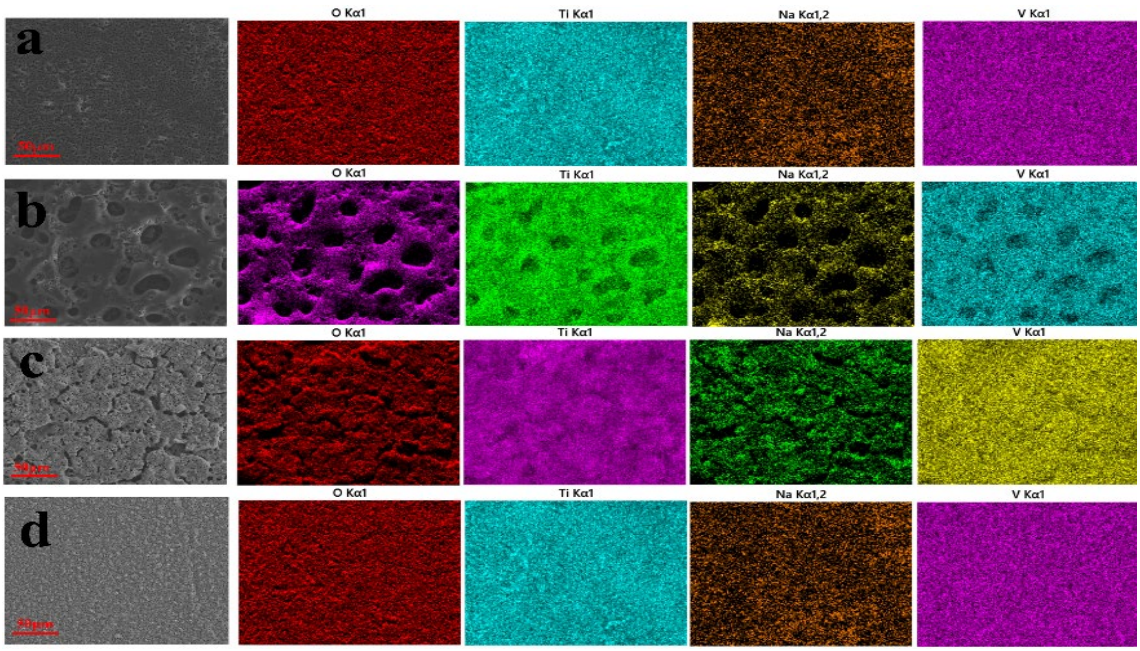

Fig. 6. SEM surface scanning of MAO layer with different Na_2S addition (a: 0 g/L, b: 10 g/L, c: 20 g/L, d: 30 g/L).

Fig.7 is the friction test results of MAO coatings with different Na_2S content. It can be seen that the addition of Na_2S has no obvious effect on the friction performance of the film. The friction curves show a trend of rapid decline after slow growth. When the Na_2S content is 20 g/L, the friction curve decreases first, and there is no obvious difference between 10 g/L and 30 g/L. As shown in Fig.8, with the gradual increase of Na_2S content, the average friction coefficient of MAO layer increased slightly but there was no significant difference, only increased to 0.43 at 30 g/L. There was no significant difference in the friction coefficient when the Na_2S content was 0-20 g/L, but the wear rate changed significantly. When the Na_2S content is 0 g/L, the maximum wear rate reaches 7.942×10^{-4} $mm^3/N \cdot m$.

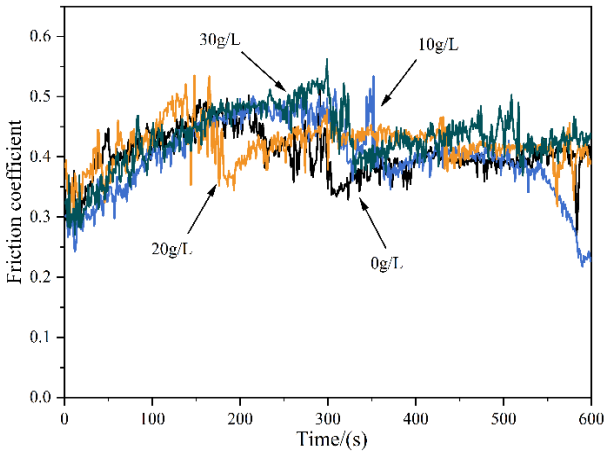

Fig. 7. Friction coefficient curves of micro-arc oxidation coatings prepared with different Na_2S additions.

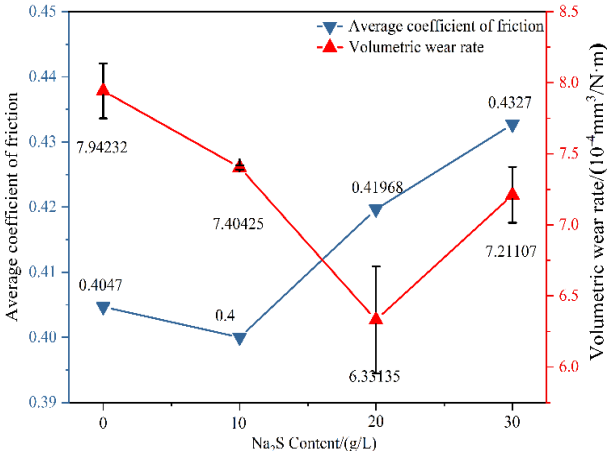

Fig. 8. Statistical figures of average friction coefficient and volume wear of MAO coatings prepared with different Na_2S additions.

With the increase of Na_2S content, the wear rate decreases first and then increases. When the Na_2S content is 20 g/L, the minimum is about 6.331×10^{-4} $mm^3/N \cdot m$, which may be related to the earliest decrease of friction curve when the Na_2S content is 20 g/L. On the other hand, the surface quality of MAO layer is the best when the Na_2S content is 20 g/L, so the wear resistance is the best. The increase of wear rate and friction coefficient at 30 g/L may be related to the limited growth of MAO layer and less hard phase and lubrication phase. It can be seen that due to the lack of lubricating phase, although the friction coefficient and wear rate of MAO layer with different Na_2S content have changed, the overall is still high. The improvement of friction coefficient and wear rate may be due to the improvement of surface quality caused by discharge optimization and the increase of Rutile-TiO_2 content.

Theoretically, the lattice mismatch between VS_x and TiO_2 is large, and there are many dislocations and distortions at the interface to form an incoherent interface. Incoherent interfaces may hinder the movement of dislocations, alleviate lattice strain, and reduce inter facial free energy [27], resulting in moderate interfacial bonding strength [28,29]. Therefore, the incoherent interface formed by in-situ synthesized VS_x improves the mechanical properties of the ceramic coating. As shown in Fig.9, at the micro level, this incoherent interface hinders the dislocation motion near the VS_x phases, which enables VS_x to be fixed in the ceramic layer, ensuring that VS_x can provide wear resistance for long duration.

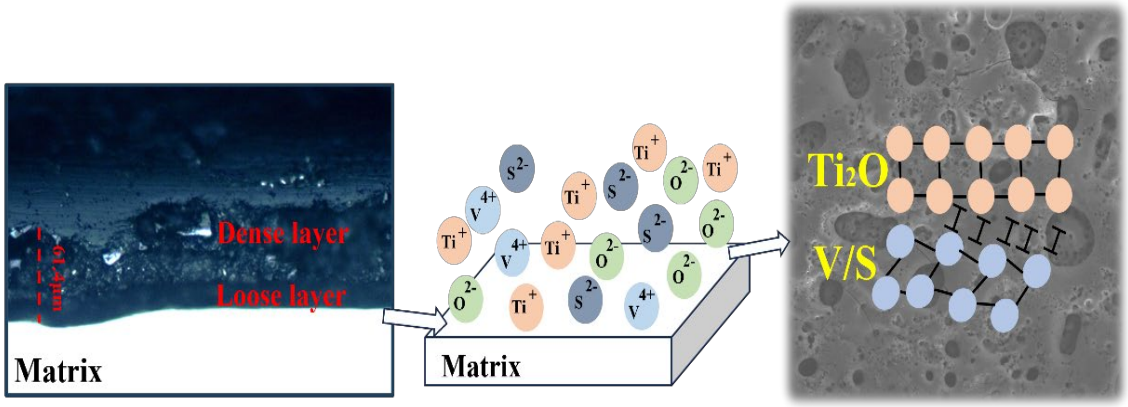

Fig. 9. Incoherent interface between VS_x and TiO_2.

4. Conclusions

A composite MAO layer containing VS_x/TiO_2 phase was in-situ prepares on the TC4 alloy surface by MAO process. Four concentrations of Na_2S (0 g/L, 10 g/L, 20 g/L and 30 g/L) were used as variables of electrolyte composition. It is concluded that: (1) the VS_x phases can be formed on the surface layer by adding Na_2S into Na_3VO_4. (2) With the increase of Na_2S content, the pores and cracks on the MAO surface increase first and then decrease. The layer is uniform and dense when the addition of Na_2S is 30 g/L, and the layer has the least micropores, and the lowest roughness. (3) When the Na_2S content is 20 g/L, the average friction coefficient is 0.419 and the volume wear rate is 6.331×10^{-4} $mm^3/N \cdot m$. (4) The appropriate concentration of Na_2S in present work is 10-20 g/L.

References

[1] B.Y. Xie, K. Gao, Coatings.13(9) (2023)1486; https://doi.org/10.3390/coatings13091486
[2] J.S. Zhang, Y. Pan, Q.J. Zhou, J.Z. Sun, Y.J. Liu, F. Kuang, C.X. Lei, X. Lu, Mater. Today. Commun.37(2023)106952; https://doi.org/10.1016/j.mtcomm.2023.106952
[3] L.Y. Chen, Y.W. Chen, L.C. Zheng, Metals.10(9) (2020)1139; https://doi.org/10.3390/met10091139
[4] T.L. Zhang, J.M. Zhu, T. Yang, J.H. Luan, H.J. Kong, W.H. Liu, B.X. Cao, S.W. Wu, D. Wang, Y.Z. Wang, S. Liu, Scr. Mater.207(2022)114260; https://doi.org/10.1016/j.scriptamat.2021.114260
[5] Y. Pan, J.S. Zhang, X.X. Wu, Y.C. Yang, F. Kuang, C. Zhang, D. Lu, X. Lu, J. Alloy. Compd. 939 (2023)168686; https://doi.org/10.1016/j.jallcom.2022.168686
[6] L. Li, M.Q. Li, Prog. Nat. Sci.32(4) (2022) 490–497; https://doi.org/10.1016/j.pnsc.2022.07.007
[7] X. Lu, Y. Pan, W.B. Li, M.D. Hayat, F. Yang, H. Singh, W.W. Song, X.H. Qu, Y. Xu, P. Cao, Mater. Sci. Eng. A.795 (2020)139924; https://doi.org/10.1016/j.msea.2020.139924
[8] Z.D. Liu, Z.X. Du, H.Y. Jiang, T.H. Gong, X.M. Cui, J.W. Liu, J. Cheng, Prog. Nat. Sci.31(5) (2021)731–741; https://doi.org/10.1016/j.pnsc.2021.08.008
[9] G.T. Liu, K. Leng, X.H. He, L.N. Tang, W.H. Gao, Y.D. Fu, Prog. Nat. Sci.32(4) (2022)424–432; https://doi.org/10.1016/j.pnsc.2022.06.004
[10] W.J. Lu, D. Zhang, X.N. Zhang, R.J. Wu, T. Sakata, H. Mori, J. Alloys Compd. 327(1-2)(2001)240–247; https://doi.org/10.1016/S0925-8388(01)01445-1
[11] A. Panigrahi, M. Bönisch, T. Waitz, E. Schafler, M. Calin, J. Eckert, W. Skrotzki, M. Zehetbauer, J. Alloys Compd.628(2015) 434–441; https://doi.org/10.1016/j.jallcom.2014.12.159
[12] H. Attar, K.G. Prashanth, A.K. Chaubey, M. Calin, L.C. Zhang, S. Scudino, J. Eckert, Mater. Lett.142(2015)38–41; https://doi.org/10.1016/j.matlet.2014.11.156
[13] S.E. Haghighi, H.B. Lu, G.Y. Jian, G.H. Cao, D. Habibi, L.C. Zhang, Mater. Des. 76(2015)47–54; https://doi.org/10.1016/j.matdes.2015.03.028

[14] Y. Xu, P.Z. Xia, Y.Q. Cai, Z.Y. Wei, S.T. Zhao, Dig. J. Nanomater. Biostructures. 17(1)(2022)301-316; https://doi.org/10.15251/DJNB.2022.171.301
[15] J.D. Cotton, R.D. Briggs, R.R. Boyer, S. Tamirisakandala, P. Russo, N. Shchetnikov, J.C. Fanning, JOM.67(6)(2015)1281–1303; https://doi.org/10.1007/s11837-015-1442-4
[16] A.S. Bychkov, V.N. Fedirko, Mater. Sci.52(2016)9–16; https://doi.org/10.1007/s11003-016-9920-6
[17] Q. Jun, J.B. Peter, R.W. Thomas, B.C. Odis, S.K. Nagraj, Wear. 258(9) (2005) 1348-1356; https://doi.org/10.1016/j.wear.2004.09.062
[18] Q.Y. Zhang, Y. Zhou, L. Wang, X.H. Cui, S.Q. Wang, Tribol. Int. 94(2016)541-549; https://doi.org/10.1016/j.triboint.2015.10.018
[19] H.G. Jeong, Y. Lee, D.G. Lee, Surf. Coat. Technol. 326(2017)395–401; https://doi.org/10.1016/j.surfcoat.2017.01.003
[20] C.D.S. Tousch, L. Magniez, S. Fontana, G. Marcos, C. Herold, G. Henrion, T. Czerwiec, J. Martin, Surf.Coat.Technol.468(2023)129779; https://doi.org/10.1016/j.surfcoat.2023.129779
[21] E. Arslan, Y. Totik, E.E. Demirci, Y. Vangolu, A. Alsaran, I. Efeoglu, Surf.Coat.Technol. 204(6-7)(2009)829-833; https://doi.org/10.1016/j.surfcoat.2009.09.057
[22] G.Q. Li, F.C. Ma, P. Liu, S.C. Qi, W. Li, K. Zhang, X.H. Chen, J. Alloys Compd. 948(2023)169773; https://doi.org/10.1016/j.jallcom.2023.169773
[23] M. Kaseem, T. Hussain, Z.U. Rehman, Y. G. Ko, J. Alloys Compd.853(2021)157036; https://doi.org/10.1016/j.jallcom.2020.157036
[24] N. Xiang, R.G. Song, B. Xiang, H. Li, Z.X. Wang, C. Wang, Appl. Surf. Sci. 347(2015)454-460; https://doi.org/10.1016/j.apsusc.2015.04.136
[25] B.S. Lou, J.W. Lee, C.M. Tseng, Y.Y. Tseng, C.A. Yen, Lin, Surf. Coat. Technol.350(2018) 813–822; https://doi.org/10.1016/j.surfcoat.2018.04.044
[26] G.Y. Gu, J. Shang, X.Y. Zhang, Chalcogenide Lett.19(2022)955-964; https://doi.org/10.15251/CL.2022.1912.955
[27] Z. Yang, Z. Zhang, Y.N. Chen, Q.Y. Zhao, Y.K. Xu, F.Y. Zhang, H.F. Zhan, S.P. Wang, H.Z. Li, J.M. Hao, Y.Q. Zhao, Scripta Materialia, 211(2022)114493; https://doi.org/10.1016/j.scriptamat.2021.114493
[28] D.Q. Liu, A.J. Zhang, J.G. Jia, J.S. Han, J.Y. Zhang, J.H. Meng, Compos. B. Eng.212 (2021) 108681; https://doi.org/10.1016/j.compositesb.2021.108681
[29] X.L. Han, P. Liu, D.L. Sun, Q. Wang, Compos. B. Eng.185(2020)107794; https://doi.org/10.1016/j.compositesb.2020.107794